

Absence of Magnetism in Hcp Iron-Nickel at 11 K

A. B. Papandrew, M. S. Lucas, R. Stevens, I. Halevy, and B. Fultz

Division of Engineering and Applied Science, MC 138-78, California Institute of Technology, Pasadena, California 91125, USA

M. Y. Hu and P. Chow

HP-CAT, Carnegie Institution of Washington, Advanced Photon Source, Argonne National Laboratory, Argonne, Illinois 60439, USA

R. E. Cohen and M. Somayazulu

Geophysical Laboratory, Carnegie Institution of Washington, Washington, D.C. 20015, USA

(Received 14 February 2006; revised manuscript received 19 May 2006; published 21 August 2006)

Synchrotron Mössbauer spectroscopy (SMS) was performed on an hcp-phase alloy of composition $\text{Fe}_{92}\text{Ni}_8$ at a pressure of 21 GPa and a temperature of 11 K. Density functional theoretical calculations predict antiferromagnetism in both hcp Fe and hcp Fe-Ni. For hcp Fe, these calculations predict no hyperfine magnetic field, consistent with previous experiments. For hcp Fe-Ni, however, substantial hyperfine magnetic fields are predicted, but these were not observed in the SMS spectra. Two possible explanations are suggested. First, small but significant errors in the generalized gradient approximation density functional may lead to an erroneous prediction of magnetic order or of erroneous hyperfine magnetic fields in antiferromagnetic hcp Fe-Ni. Alternately, quantum fluctuations with periods much shorter than the lifetime of the nuclear excited state would prohibit the detection of moments by SMS.

DOI: [10.1103/PhysRevLett.97.087202](https://doi.org/10.1103/PhysRevLett.97.087202)

PACS numbers: 75.50.Ee, 61.18.Fs, 71.15.Mb, 74.62.Fj

Elemental iron, which has the body-centered cubic (bcc) crystal structure at ambient temperature and pressure, transforms to the hexagonal-close packed (hcp) phase at a pressure of approximately 13 GPa. The properties of hcp Fe are important for understanding the geophysics of the core of the Earth and for understanding the propagation of high-pressure shock waves through engineering materials. An antiferromagnetic (AFM) ground state has been predicted repeatedly for the hcp ϵ phase of iron [1–8], but, in the nearly 50 years since ϵ -Fe was first synthesized [9], Mössbauer effect experiments have never detected the presence of a hyperfine magnetic field (HMF) [10–12], implying the absence of static magnetic moments or magnetic order. Recent density functional theory (DFT) calculations have suggested that the vanishing HMF in hcp iron can be explained by cancellation of a large core electron polarization by an equally large itinerant electron polarization in the *afmII* antiferromagnetic state [1,5,6]. This hypothesis neatly explains the null results of the Mössbauer measurements but sustains the possibility of antiferromagnetism in ϵ -iron. DFT calculations for the *afmII* structure have shown markedly better agreement with equation of state and elasticity measurements than nonmagnetic calculations [5] and have provided an explanation for the split Raman mode in ϵ -Fe [13] and a consistent calculation of this splitting [6]. These findings, taken together with the recent discovery of an unusual form of superconductivity in ϵ -Fe [14], lend new importance to determination of the correct magnetic ground state of ϵ -Fe, a topic with considerable history.

In the present work, we tested the idea that ϵ -iron is antiferromagnetic yet exhibits no hyperfine field owing to

the cancellation of up and down spin densities at iron nuclei. If indeed a delicate balance between core and conduction electron polarization exists, a magnetic perturbation should disrupt it, producing measurable hyperfine magnetic fields. Local hyperfine magnetic field perturbations at ^{57}Fe atoms caused by impurities have been thoroughly investigated by Mössbauer [15–17] and NMR [18] spectrometry measurements on iron-rich bcc alloys. Transition metal solutes such as nickel cause increases of the magnetic moments at neighboring iron atoms, altering their core electron polarizations [15,17,19]. In addition, the altered magnetic moment at the solute site causes a redistribution of spin density of the conduction electrons. Hyperfine magnetic fields at iron atoms with nickel neighbors in bcc alloys differ by tens of kiloGauss with respect to pure iron. Mössbauer spectroscopy techniques are able to resolve HMF values of approximately 10 kG, and smaller effects can be detected from the broadening of spectral lines. We expect that, in the case of static magnetic moments, an hcp iron alloy dilute in nickel with the *afmII* spin structure will exhibit local environments with non-negligible hyperfine magnetic fields.

An alloy of nominal composition $\text{Fe}_{92}\text{Ni}_8$ was made by arc-melting iron of 99.99% purity with 20% enrichment in ^{57}Fe and natural nickel of 99.98% purity in an argon atmosphere. No mass loss was detected, and electron microprobe measurements established an actual composition of $\text{Fe}_{0.929}\text{Ni}_{0.071}$. The resulting ingot was then rolled to a thickness of 50 μm . X-ray diffractometry with $\text{Cu } K_\alpha$ radiation showed a uniform bcc structure with (2 0 0) texture and a lattice parameter almost identical to that of pure iron. A series of energy-dispersive x-ray diffraction

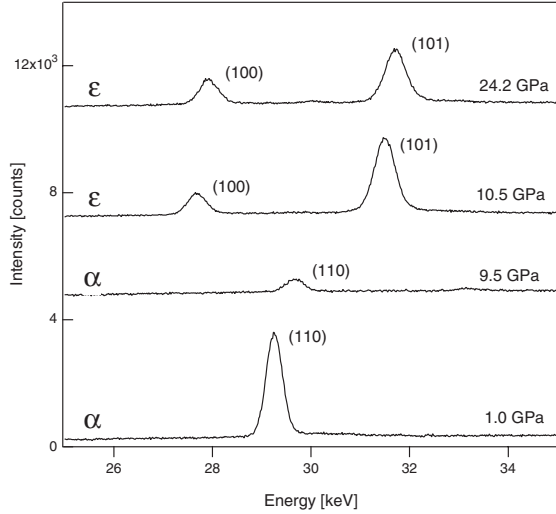


FIG. 1. Selected energy-dispersive x-ray diffraction patterns from $\text{Fe}_{92}\text{Ni}_8$ from 1–24 GPa. The alloy transformed from the α phase to the ϵ phase between 9 and 10 GPa.

(EDXRD) patterns were measured at beam line X-17C of the National Synchrotron Light Source to identify the pressure of the $\alpha \rightarrow \epsilon$ phase transition. The sample was loaded in a Merrill-Bassett diamond anvil cell (DAC) [20] with diamonds having 500 μm culets, silicone oil as the pressure medium, and 301 stainless steel as a gasket material. The ruby fluorescence technique was used for pressure determination [21]. The EDXRD patterns (Fig. 1) showed that the $\alpha \rightarrow \epsilon$ phase transition occurred at approximately 10 GPa. No bcc diffraction peaks were detected at pressures higher than 14 GPa. The $(1\ 1\ 0)\alpha$ peak is clearly visible at 9.5 GPa but disappears at 10.1 GPa and coincides with the appearance of the $(1\ 0\ 0)\epsilon$ and $(1\ 0\ 1)\epsilon$ peaks. The $(2\ 0\ 0)\epsilon$ peak is weak, typical of effects from crystallographic texture.

Full-potential DFT linearized augmented plane wave (LAPW) calculations were performed in the generalized gradient approximation (GGA) [22] with the WIEN2K software package [23]. A 16 atom supercell belonging to the $Pm\bar{m}a$ space group was constructed for the composition Fe_7Ni_1 (Fig. 2), and some computations were performed for a 16 atom cell of composition $\text{Fe}_{15}\text{Ni}_1$. For Fe_7Ni_1 , an $11 \times 8 \times 5$ special k -point mesh was used, containing 500 k points in the Brillouin zone and 72 points in the irreducible wedge. A muffin-tin radius R_{MT} of 2.0 au was used, and $R_{\text{MT}}K_{\text{max}}$ was 8. Spin-polarized total energy calculations were performed for the $afmII$ structure, for which spins were assigned according to the scheme of Steinle-Neumann *et al.* [6] and are also shown in Fig. 2. Unpolarized calculations were also performed for the nonmagnetic structure. Total energies were computed for a range of cell volumes and the resulting energy-volume curves fitted to the third-order Birch Murnaghan equation of state.

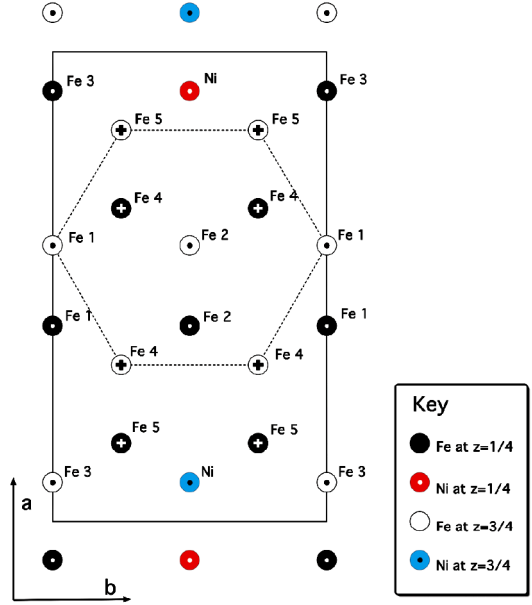


FIG. 2 (color online). The Fe_7Ni_1 supercell with the $afmII$ spin structure [6]. Crosses denote a spin orientation pointing into the page, while circles indicate spin pointing out of the page.

The calculations on the $Pm\bar{m}a$ Fe_7Ni_1 supercell showed that the $afmII$ (AFM) structure is more stable than its ferromagnetic or nonmagnetic (NM) counterparts at a pressure of 21 GPa at 0 K. We calculated a total energy difference of 3.5 mRy per atom between the two states at their zero-pressure volumes (71.5 and 69.2 au^3/atom for AFM and NM, respectively) and a difference of 2.4 mRy at 21 GPa (65.5 and 64.6 au^3/atom for AFM and NM, respectively). Hyperfine magnetic fields (HMFs) were calculated for the AFM structure and are tabulated in Table I. The largest HMFs were from Fe atoms neighboring the Ni atom, and this same result was found for $\text{Fe}_{15}\text{Ni}_1$. Disordered systems could be studied using the coherent potential approximation (CPA) [24], but that would not allow us to examine the importance of proximity of the Fe to the Ni atoms. Real space methods such as the locally self-consistent multiple scattering (LSMS) method [25] would allow such information to be obtained, but a full-potential implementation would be necessary, and full-potential versions are not yet completely tested. We used

TABLE I. HMF at ^{57}Fe in ϵ -phase $afmII$ Fe_7Ni_1 (65.5 au^3/atom) and ϵ -phase $afmII$ Fe (65 au^3/atom).

Atom	B_{val} [kG]	B_{core} [kG]	B_{tot} [kG]
Pure Fe	89	-85	4
Fe 1 in Fe_7Ni_1	133	-108	25
Fe 2 in Fe_7Ni_1	117	-107	10
Fe 3 in Fe_7Ni_1	130	-91	39
Fe 4 in Fe_7Ni_1	-85	109	24
Fe 5 in Fe_7Ni_1	-102	168	66

the supercell method, and the fact that we obtain the same results for two supercells of very different composition suggests strongly that CPA or LSMS would also predict a magnetic state with noncancelling HMFs.

Synchrotron Mössbauer spectrometry (SMS) experiments were performed at beam line 16 ID-D of the High-Pressure Collaborative Access Team (HP-CAT) at the Advanced Photon Source. A symmetric piston-cylinder type diamond anvil cell was employed with diamonds of 500 μm culet diameter. A rhenium gasket contained the sample and the silicone oil pressure medium. The sample was compressed to 20.8 GPa as measured by ruby fluorescence. The DAC was installed in the cold head of a Cryo-Industries ^4He flow cryostat that was mounted on the positioning stage of 16 ID-D. Synchrotron Mössbauer spectroscopy measurements were made by counting the delayed, coherent products of nuclear deexcitation as a function of time. The synchrotron ring was operated in top-up singlet mode with 153 ns bunch separation. A silicon high-resolution monochromator delivered 2 meV bandwidth. Spectra were recorded at ambient temperature (296 K) and at 11 K, as monitored within the cryostat by a pair of diodes, located at the capillary orifice and at the sample.

The SMS spectra from a sample at ambient pressure and temperature show the quantum beats expected from the ferromagnetic α phase superimposed on a dynamical beat pattern resulting from the large effective thickness of the sample (Fig. 3). The time spectra from the pressurized sample exhibit only dynamical beats at both 296 and 11 K (and for a different sample at 77 K). Using the program CONUSS [26], theoretical curves were fit to the measured data. The best fits to the ϵ -phase data were obtained when the hyperfine magnetic field parameter

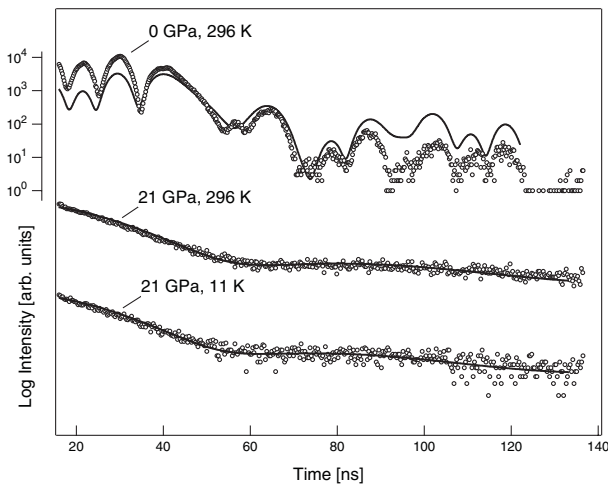


FIG. 3 (color online). SMS spectra from $\text{Fe}_{92}\text{Ni}_8$ at various temperatures and pressures. The numerical scale applies only to the topmost curve and is provided as a reference. Solid lines are theoretical fits to the data. At 0 GPa and 296 K, the sample is bcc. At 21 GPa, it is hcp.

was set to zero. The HMF distribution in Table I was input to CONUSS to generate the expected SMS spectrum for *afmII* Fe_7Ni_1 and $\text{Fe}_{15}\text{Ni}_1$ at 20 GPa. The results for Fe_7Ni_1 are compared to the experimental SMS spectrum in Fig. 4. The calculated HMF would modulate substantially the SMS spectrum, but this is not seen in the data.

One possible explanation of the lack of an observed HMF would be if the Néel temperature T_N is below the measurement temperature of 11 K. We obtained an estimate of T_N using a multiscale approach for pure iron [27]. We used a tight-binding model that was fit to LAPW calculations within the GGA [1,28] to compute the energies for 93 different magnetic configurations and moments for 4 and 64 atom supercells. Parameters of an extended Heisenberg model [29] were fit to the total energies, and classical Monte Carlo (MC) simulations were performed on a 512 atom hcp supercell. We obtain $T_N = 350$ K at 70 au^3/atom , 75 K at 65 au^3/atom , and 0 K (only very small moments are present) at 60 au^3/atom . The corresponding pressures for the theoretical equation of state are 0, 21, and 55 GPa. Diffraction data on our sample gives a volume of 70.85 au^3 at 19 GPa ($a = 2.468$ Å, $c = 3.977$ Å). The MC results suggest strongly that the measurement temperature of 11 K should be below T_N . The possibility remains that geometrical frustration in hcp leads to a degenerate ground state that would be sampled by quantum fluctuations at low T [30].

This leaves two apparent explanations of the results. The first is that the GGA functional is overestimating the exchange coupling in hcp Fe, predicting incorrectly the magnetic order. The errors could not be too large, because the transition pressure from magnetic bcc to hcp is well-predicted by the GGA [7]. We find that a 20% decrease in

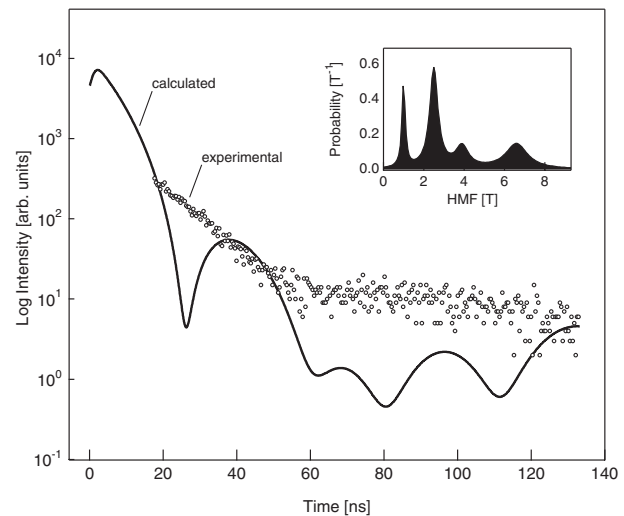


FIG. 4. Experimental data from hcp $\text{Fe}_{92}\text{Ni}_8$ at 11 K and a simulated SMS spectrum generated with CONUSS based on DFT calculations of HMF in Fe_7Ni_1 . Inset: The HMF distribution for the simulated spectrum.

the effective Stoner exchange parameter I from the fitted value of $1.0746 \text{ eV}/\mu_B$ to 0.90 gives a drop in moment from $1.077\mu_B$ per atom to 0.053 at $70 \text{ au}^3/\text{atom}$. An overestimate of the exchange coupling by 20% by the GGA does not seem unreasonable.

Alternatively, quantum spin fluctuations [31,32] in ϵ -iron may be too fast for the Mössbauer time window of a few nanoseconds, inhibiting detection of a hyperfine field. FeAl presents a similar case, where DFT predicts a magnetic ground state not observed experimentally; dynamical mean field theory computations correctly give a paramagnetic ground state due to spin fluctuations [32]. Also, the hcp lattice is geometrically frustrated with respect to antiferromagnetism, and it is known that fluctuations play an important role in the physics of many frustrated antiferromagnets [33,34]. Spin fluctuation rates in the gigahertz range have been identified in these materials and cannot be discounted for ϵ -Fe. (A third possibility is that a chemically disordered Fe-Ni alloy, unlike the ordered supercell we studied, has precise cancellations of its HMF's. We believe this unlikely, given the consistency of results from different supercells and the local nature of the effects of Ni atoms on the ^{57}Fe HMF. Future computations using CPA, LSMS, or related methods could test this.)

Our results suggest that hcp iron-nickel, and possibly pure hcp iron, do not have static antiferromagnetism, contrary to predictions of DFT. The ability of solute atoms to disrupt electron spin density at neighboring atoms suggests that there is no magnetic structure to disrupt. The possibility remains that quantum spin fluctuations are occurring on a time scale faster than our experimental measurements. Such fluctuations could explain the apparent greater accuracy of magnetic DFT computations over nonmagnetic computations for elastic properties and for the observed Raman splitting and superconductivity.

We thank I. Mazin, D. Singh, and G. Steinle-Neumann for helpful discussions and H. P. Liermann for assistance with the SMS experiments. This work was supported by the Carnegie-DOE Alliance Center, funded by the Department of Energy through the Stewardship Sciences Academic Alliance Program under Grant No. DE-FC03-03NA00144, and by DOE ASCI/ASAP Subcontract No. B341492 to Caltech DOE No. W-7405-ENG-48 (R. E. C.). Use of the Advanced Photon Source is supported by the U.S. Department of Energy under Contract No. W-31-109-ENG-38.

-
- [1] R. E. Cohen and S. Mukherjee, Phys. Earth Planet. Inter. **143/144**, 445 (2004).
 [2] J. Goniakowski and M. Podgorny, Phys. Rev. B **44**, 12 348 (1991).

- [3] H. Ohno and M. Mekata, J. Phys. Soc. Jpn. **31**, 102 (1971).
 [4] H. Ohno, J. Phys. Soc. Jpn. **31**, 92 (1971).
 [5] G. Steinle-Neumann, R. E. Cohen, and L. Stixrude, J. Phys. Condens. Matter **16**, S1109 (2004).
 [6] G. Steinle-Neumann, L. Stixrude, and R. E. Cohen, Proc. Natl. Acad. Sci. U.S.A. **101**, 33 (2004).
 [7] L. Stixrude, R. E. Cohen, and D. J. Singh, Phys. Rev. B **50**, 6442 (1994).
 [8] V. Thakor *et al.*, Phys. Rev. B **67**, 180405(R) (2003).
 [9] D. Bancroft, E. Peterson, and S. Minshall, J. Appl. Phys. **27**, 291 (1956).
 [10] G. Cort, R. Taylor, and J. Willis, J. Appl. Phys. **53**, 2064 (1982).
 [11] S. Nasu, T. Sasaki, T. Kawakami, T. Tsutsui, and S. Endo, J. Phys. Condens. Matter **14**, 11 167 (2002).
 [12] R. Taylor, G. Cort, and J. Willis, J. Appl. Phys. **53**, 8199 (1982).
 [13] S. Merkel, A. Goncharov, H. Mao, P. Gillet, and R. Hemley, Science **288**, 1626 (2000).
 [14] K. Shimizu *et al.*, Nature (London) **412**, 316 (2001).
 [15] M. Stearns, Phys. Rev. B **4**, 4081 (1971).
 [16] I. Vincze and G. Grüner, Phys. Rev. Lett. **28**, 178 (1972).
 [17] I. Vincze and I. Campbell, J. Phys. F **3**, 647 (1973).
 [18] P. C. Riedi, Phys. Lett. A **33**, 273 (1970).
 [19] B. Fultz and J. W. Morris, Jr., Phys. Rev. B **34**, 4480 (1986).
 [20] E. Sterer, M. Pasternak, and R. Taylor, Rev. Sci. Instrum. **61**, 1117 (1990).
 [21] R. A. Forman, G. J. Piermarini, J. D. Barnett, and S. Block, Science **176**, 284 (1972).
 [22] J. P. Perdew, K. Burke, and M. Ernzerhof, Phys. Rev. Lett. **77**, 3865 (1996).
 [23] P. Blaha *et al.*, Comput. Phys. Commun. **59**, 399 (1990).
 [24] A. E. Kissavos, S. I. Simak, P. Olsson, L. Vitos, and I. A. Abrikosov, Comput. Mater. Sci. **35**, 1 (2006).
 [25] Y. Wang, G. M. Stocks, D. M. C. Nicholson, and W. A. Shelton, Comput. Math. Appl. **35**, 85 (1998).
 [26] W. Sturhahn and E. Gerda, Phys. Rev. B **49**, 9285 (1994).
 [27] See EPAPS Document No. E-PRLTAO-97-011635 for methods, parameters, and results from calculations of the Néel temperature of hcp Fe. The Néel temperature is well above 11 K for two atomic volumes reported. For more information on EPAPS, see <http://www.aip.org/pubservs/epaps.html>.
 [28] R. E. Cohen, L. Stixrude, and E. Wasserman, Phys. Rev. B **56**, 8575 (1997).
 [29] N. M. Rosengaard and B. Johansson, Phys. Rev. B **55**, 14 975 (1997).
 [30] R. Moessner and A. P. Ramirez Phys. Today **59**, No. 2, 24 (2006).
 [31] I. I. Mazin, D. A. Papaconstantopoulos, and M. J. Mehl, Phys. Rev. B **65**, 100511(R) (2002).
 [32] A. G. Petukhov, I. I. Mazin, L. Chioncel, and A. I. Lichtenstein, Phys. Rev. B **67**, 153106 (2003).
 [33] R. Moessner and J. T. Chalker, Phys. Rev. Lett. **80**, 2929 (1998).
 [34] S. Dunsiger *et al.*, Phys. Rev. Lett. **85**, 3504 (2000).